

## Supporting Information

### Development of a Synthesis Strategy for Sulfamethoxazole Derivatives for the Coupling to Hydrogel Microparticles

Veronika Riedl, Matthias Portius, Lara Heiser, Philipp Riedl, Torsten Jakob, Rosa Gehring, Thorsten Berg, Tilo Pompe

#### 1. Extended Experimental Section

##### 1.1 Preceding test reactions for the attempted synthesis of methyl 3-((4-((*tert*-butoxycarbonyl)amino)phenyl)-sulfonamide)isoxazole-5-carboxylate (*compound 3*)

The synthesis of methyl 3-((4-((*tert*-butoxycarbonyl)amino)phenyl)-sulfonamide)isoxazole-5-carboxylate was initially attempted according to Zhang *et al.* 4-(Boc-amino)-benzenesulfonyl chloride (20.0 mg, 68.6  $\mu\text{mol}$ , 1.0 equiv.) was dissolved in ice cold dichloromethane (DCM) (1 ml)<sup>1</sup>. Afterwards methyl-3-amino-1,2-oxazole-5-carboxylate (10.1 mg, 71.1  $\mu\text{mol}$ , 1.0 equiv.) in  $\text{NEt}_3$  (19.1  $\mu\text{l}$ , 2.0 equiv.) and DCM (126.0  $\mu\text{l}$ ) was added dropwise at 0 °C. The reaction mixture was brought to room temperature (r.t.) and stirred for 21 h. After that, the reaction mixture was washed with brine. The aqueous phase was re-extracted with DCM and dried over  $\text{MgSO}_4$ . The solvent was removed under reduced pressure to get a crude yellow solid which was purified via column chromatography (ethyl acetate/hexane, 1:1, v/v). No product could be isolated following these reaction conditions and the desired product **3** could not be obtained (Table S1, condition 1). However, the protocol was used as a starting point to optimize the reaction conditions by performing several test reactions (Table S1).

**Table S1:** Performed test reactions.

condition	base	solvent	yield of <i>compound 3</i>
1	2.0 equiv. $\text{NEt}_3$	DCM	/
2	4.0 equiv. $\text{NEt}_3$	DCM	/ <sup>a</sup>
3	1.0 equiv. $\text{NEt}_3$	THF <sup>b</sup>	/
4	$\text{NaHCO}_3$ <sup>c</sup>	$\text{H}_2\text{O}$	/
5	2.0 equiv. pyridine	THF	/
6	2.0 equiv. pyridine	DMSO	/
7	pyridine	Pyridine	/
8	pyridine <sub>anh.</sub>	pyridine <sub>anh.</sub>	22%
9	pyridine <sub>anh.</sub>	pyridine <sub>anh.</sub>	75% <sup>d</sup>

<sup>a</sup> The side product (*compound 3b*) could be isolated with a yield of 18%.

<sup>b</sup> Reaction time was increased to 3 d.

<sup>c</sup> Addition of  $\text{NaHCO}_3$  to achieve pH 8.

<sup>d</sup> 1.2 equiv. of 3-((4-((*tert*-butoxycarbonyl)amino)phenyl)-sulfonamide)isoxazole-5-carboxylate (*compound 1*) were used.

Performing the synthesis according to Zhang *et al.*, using 4-(*boc*-amino)-benzenesulfonyl chloride (80.1 mg, 274.6  $\mu\text{mol}$ , 1.0 equiv.) dissolved in DCM (8 ml), methyl-3-amino-1,2-oxazole-5-carboxylate (40.1 mg, 282.2  $\mu\text{mol}$ , 1.0 equiv.) and 4.0 equiv. of  $\text{NEt}_3$  (157.0  $\mu\text{l}$ ), led to the formation of *tert*-butyl (4-(*N,N*-diethylsulfamoyl)phenyl)carbamate (**3b**, Fig. S1), which could be isolated after purification via two subsequent rounds of column chromatography (EtOAc/hexane, 1:1, v/v and toluene/EtOAc, 9:1, v/v) with a yield of 20.3 mg (18%).

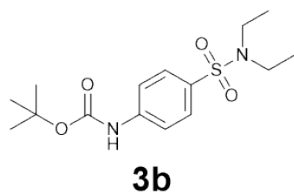


**Figure S1:** Tertiary sulfonamide product.

$^1\text{H}$  NMR (400 MHz, chloroform-*d*):  $\delta$  = 7.72 (ddd,  $J$  = 8.9, 2.6, 2.0 Hz, 2H, 7- $\text{CH}_2$ ), 7.48 (ddd,  $J$  = 8.9, 2.6, 2.0 Hz, 2H, 6- $\text{CH}_2$ ), 6.70 (s, 1H, 4-NH), 3.21 (q,  $J$  = 7.1 Hz, 4H, 9- $\text{CH}_2$ ), 1.52 (s, 9H, 1- $\text{CH}_3$ ), 1.11 (t,  $J$  = 7.1 Hz, 6H, 10- $\text{CH}_3$ ).  $^{13}\text{C}$  NMR (100 MHz, chloroform-*d*):  $\delta$  = 152.3 (3-C), 142.3 (5-C), 134.2 (8-C), 128.5 (7-C), 118.0 (6-C), 81.6 (2-C), 42.1 (9-C), 28.4 (1-C), 14.3 (10-C). MS (HR-ESI):  $m/z$  = 329.1542 (100%,  $[\text{M}+\text{H}]^+$ ), 273.0923 (86%,  $[\text{M}+\text{H}]^+-\text{C}_4\text{H}_8$ ), 200.0045 (28%,  $[\text{M}+\text{H}]^+-\text{C}_4\text{H}_8-\text{C}_4\text{H}_{10}\text{N}$ ). Calc. mass: 329.1535.

The formation of this tertiary sulfonamide product is particularly interesting, because - despite being commonly referred to as “non-nucleophilic base” - it can be assumed that triethylamine reacts as a nucleophile in this reaction. Mentions of such a reaction mechanism in literature seem to be rare. However, Matsumoto *et al.* and Gabler *et al.* described a similar phenomenon in their work<sup>2,3</sup>. Matsumoto *et al.* described the possibility of a nucleophilic aromatic substitution reaction at heteroaromatic halides using triethylamine<sup>3</sup>. In the work of Gabler *et al.* the possibility of the formation of a Meisenheimer complex intermediate is stated. The complex shall form as a result of a reaction involving triethylamine and a heteroaromatic chloride compound. However, in this case, no heteroaromatic compound was used and no Meisenheimer complex is formed as the aromaticity of the aromatic ring stays intact. On a further note, during the performed test reaction (Table S1, condition 1 and 2) a poor solubility of the amine building block (*compound 2*) in DCM could be observed. This could have favored the formation of the *compound 3b* over the desired *compound 3*.

### 1.2 Stability tests of hydrogel microparticles towards acetone and hydrochloric acid (HCl)

All centrifugation steps were performed at 1844 *g* and 20 °C for 10 min, if not stated otherwise.

For each stability assessment reaction, 1 mL of hydrogel microparticles in water (see section 2.5) was transferred to a 1.5 mL Eppendorf Tube® and centrifuged, subsequently. The supernatant was removed, and particles were washed three times with 1 mL of 4 M HCl by repeating the centrifugation step. After the last washing step, 1 mL of 4 M HCl was added once again, followed by an incubation at room temperature in a rotation shaker for 4 h. Then, the solution was centrifuged, the supernatant was removed, and particles were washed three times with 1 mL of deionized water as described above. Afterwards, the particles were analysed, see section S1.2 and S1.3). The same procedure was performed for the stability assessment of hydrogel microparticles towards acetone.

### 1.3 Bright field microscopy

The characterization of particles with regards to their structural integrity was conducted using a Leica DMI8 microscope with a HC PL FLUOTAR 20x/0.55 DRY objective. A coverslip cleaned by washing it with isopropanol and subsequently dried with nitrogen was placed in a 24-well plate with a glass bottom. The coverslips in the plate were covered with 300  $\mu\text{L}$  of HEPES buffer (pH 7.0) and 30  $\mu\text{L}$  of hydrogel microparticle solution was added. After 15 min of particle sedimentation time, hydrogel microparticles were documented. The particle diameter was determined from these images by image analysis using a home-built algorithm in Python 3.9.2 with implemented Canny Operator edge detection.

### 1.4 Reflection interference contrast microscopy

Contact areas of hydrogel microparticles were investigated using an Olympus IX73 microscope with a UPlanSApo 60x/1.35 objective. Coverslips with a diameter of 13 mm were placed in deionized water and cleaned by sonication for 30 min. Afterwards, the water was exchanged for isopropanol and the coverslips were sonicated for another 30 min twice. After the coverslip was dried with nitrogen, a 16-well plate with a rubber seal bottom was placed on the coverslip and the well was filled with 300  $\mu\text{L}$  of HEPES buffer (pH 7.0) and 25  $\mu\text{L}$  of particle solution. After a 15 min sedimentation time, contact areas were documented using Micro-Manager 2.0.0 Software<sup>4</sup>. The contact area diameter was determined from images using Fiji (ImageJ 1.53f51)<sup>5</sup>.



### 3. $^1\text{H}$ , $^{13}\text{C}$ and ESI-MS product spectra

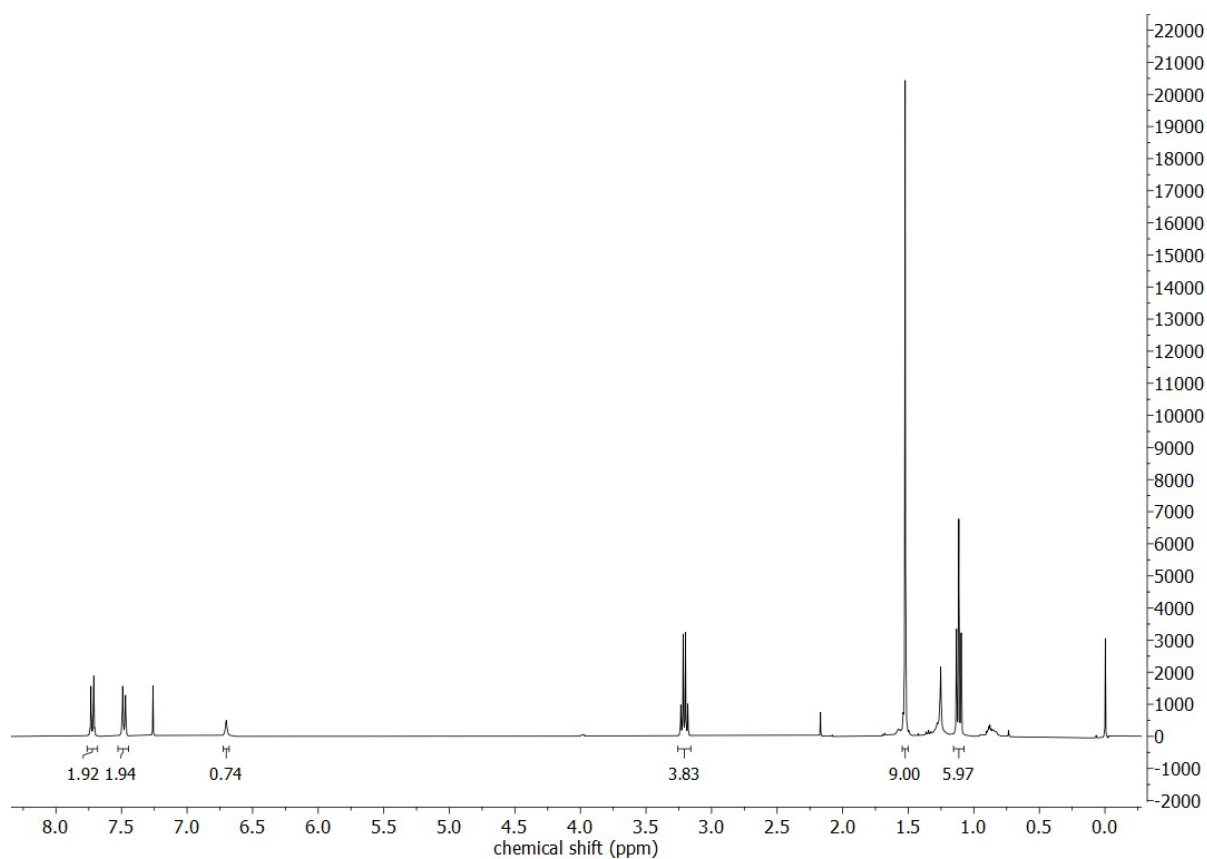


Figure S2:  $^1\text{H}$  NMR spectrum of **3b**.

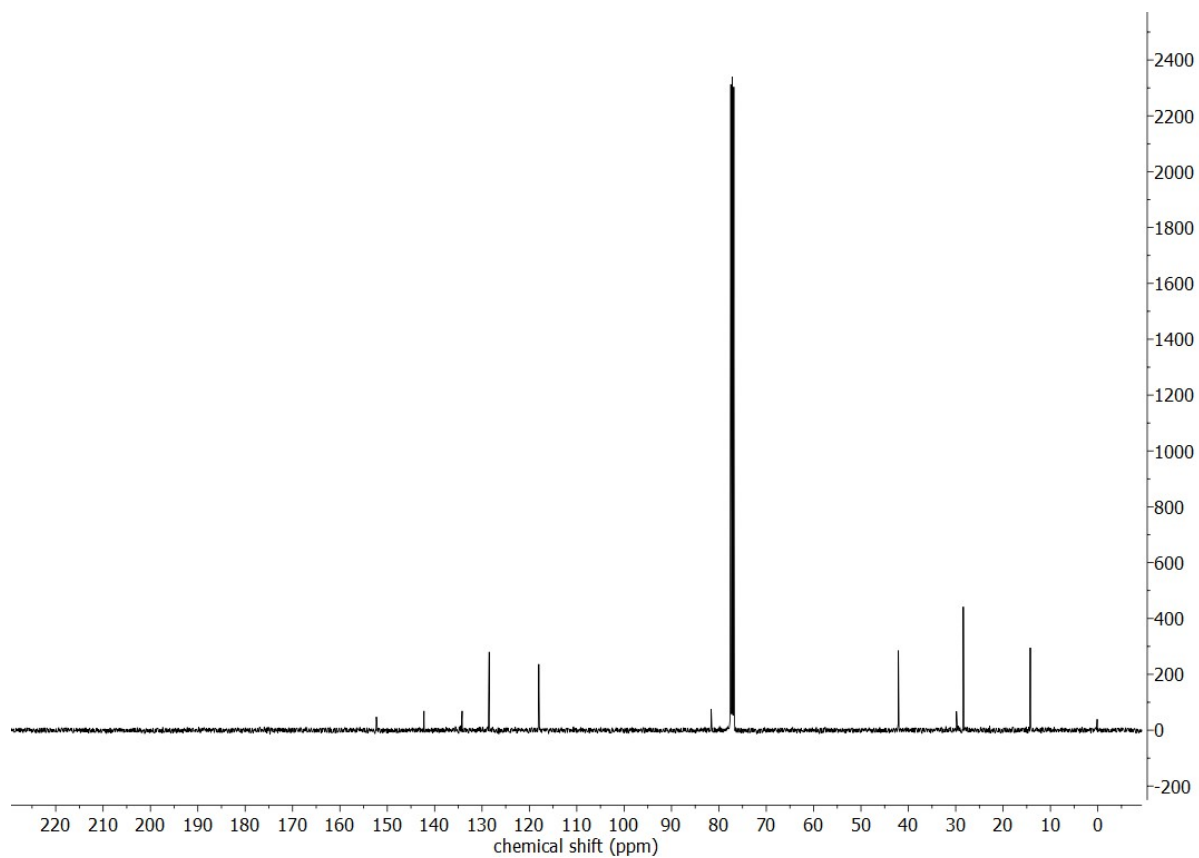
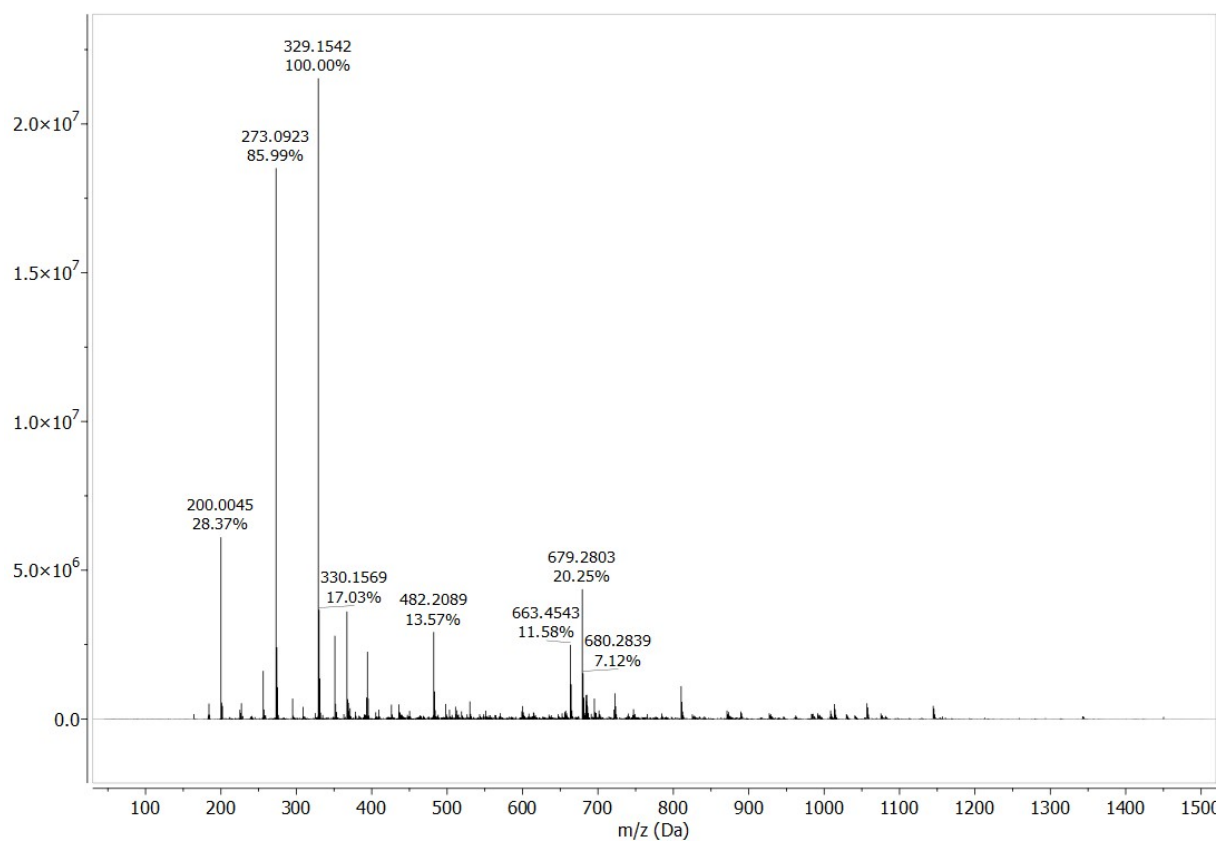
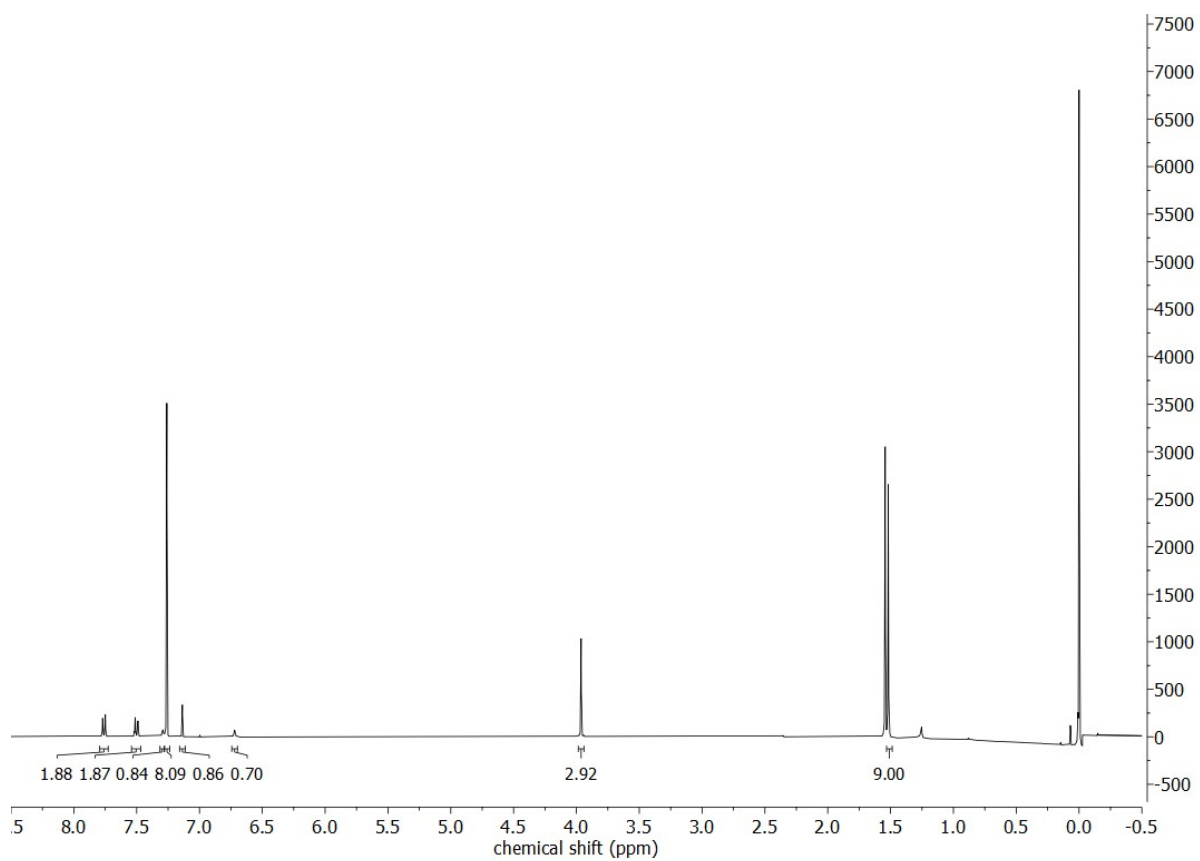


Figure S3:  $^{13}\text{C}$  NMR spectrum of **3b**.



**Figure S4:** ESI-MS (positive mode) of **3b**.



**Figure S5:**  $^1\text{H}$  NMR spectrum of **3**.

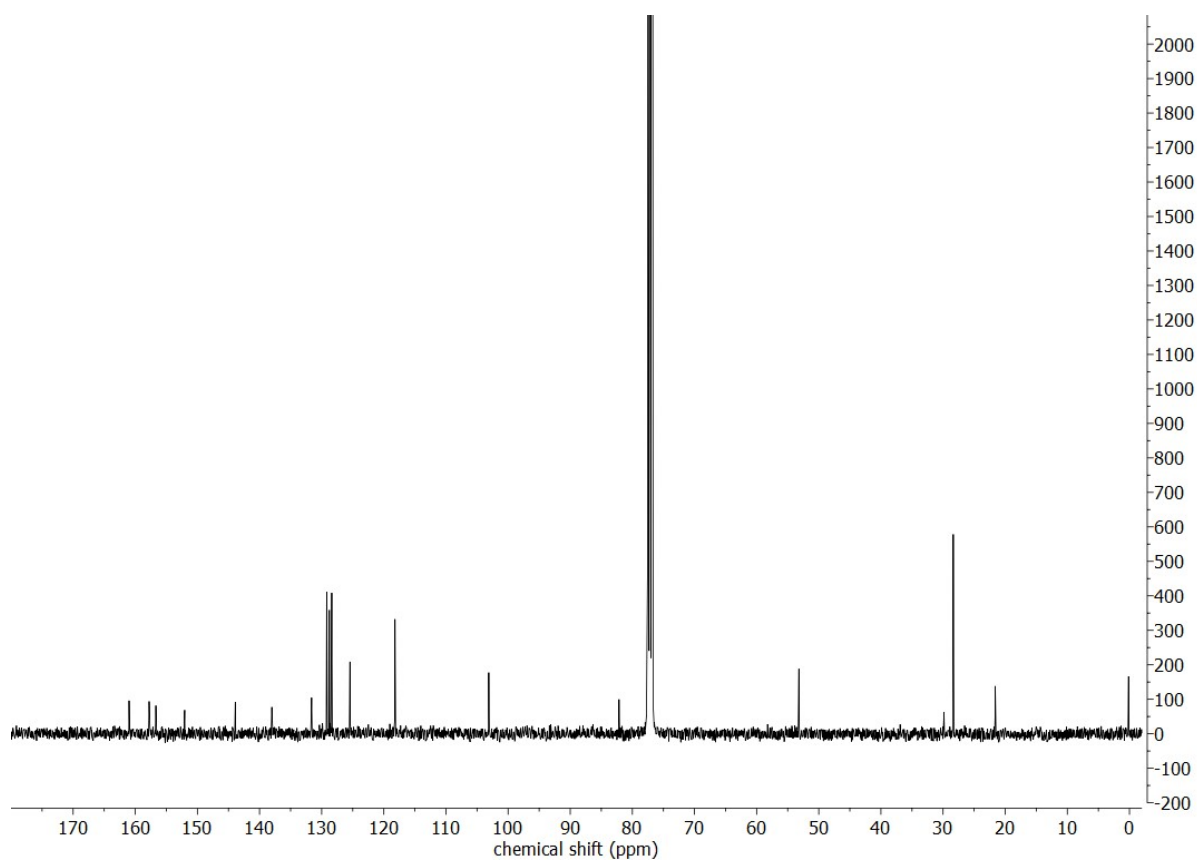


Figure S6:  $^{13}\text{C}$  NMR spectrum of **3**.

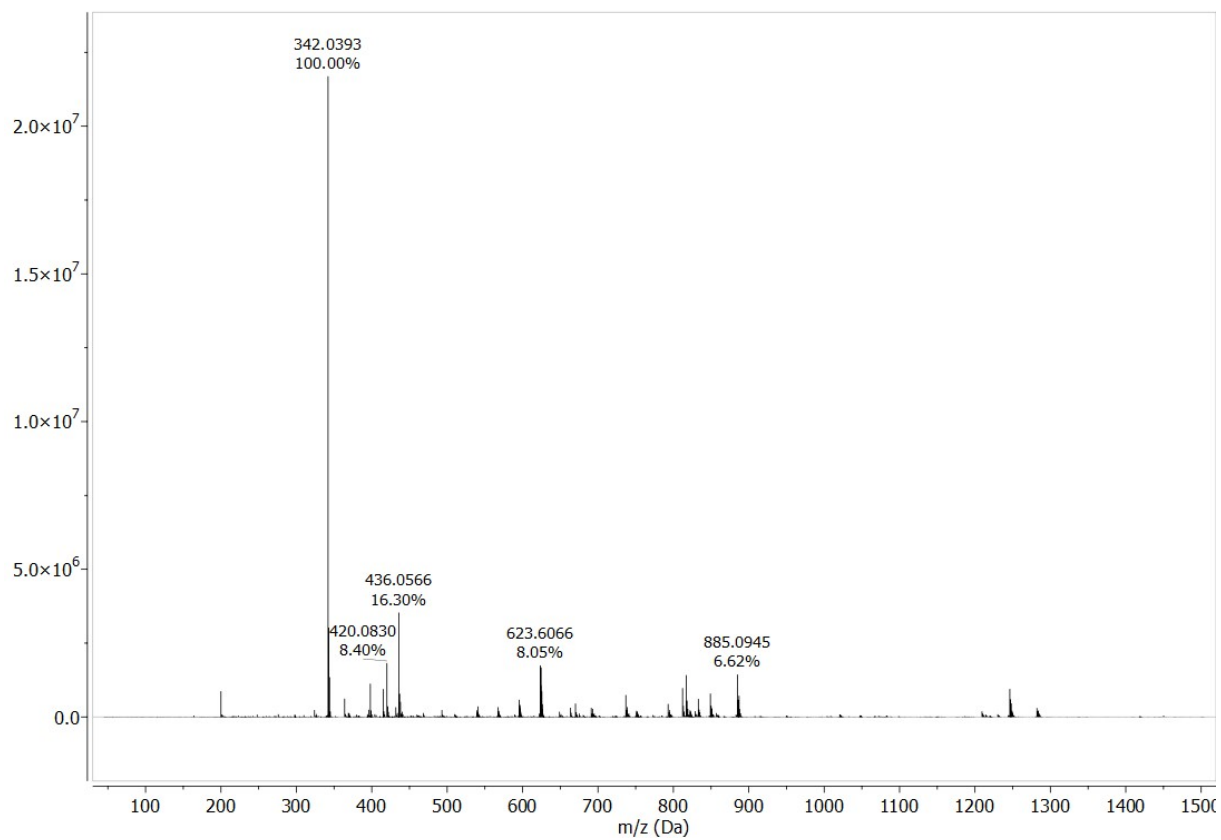
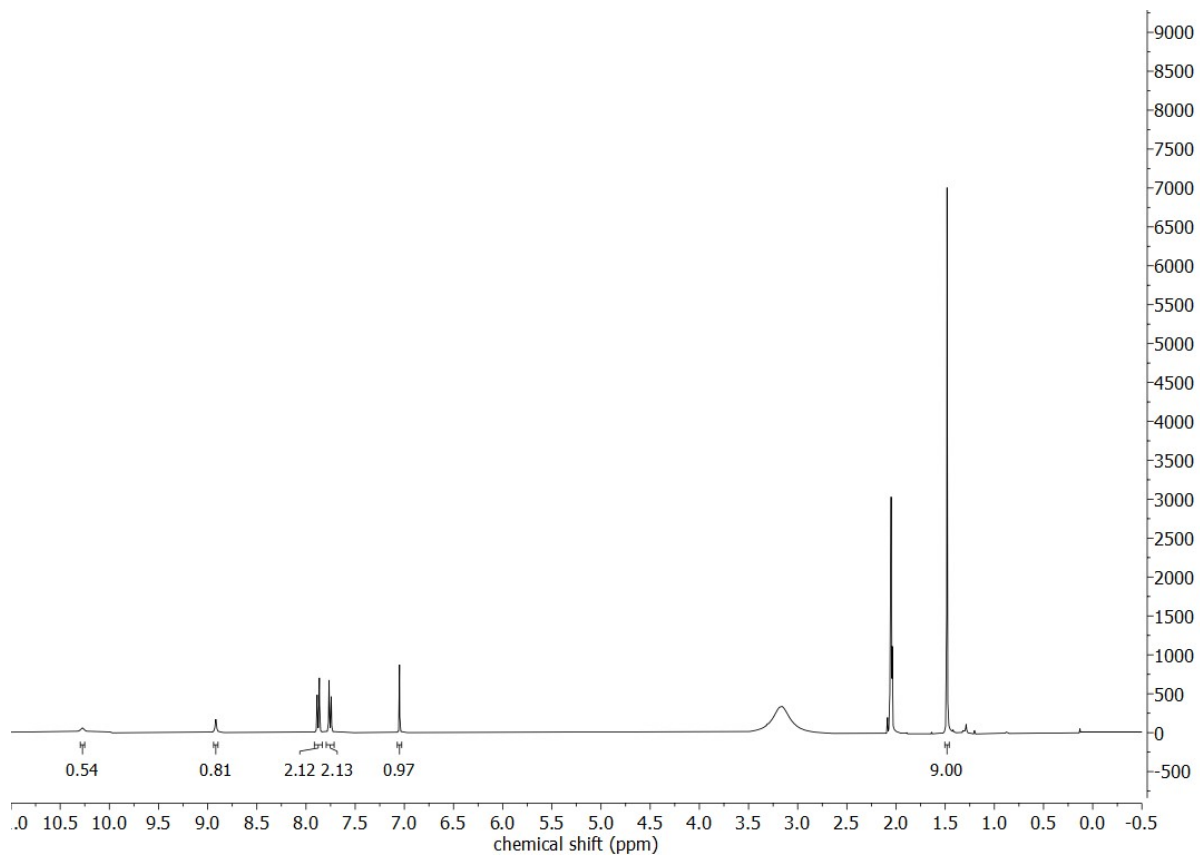
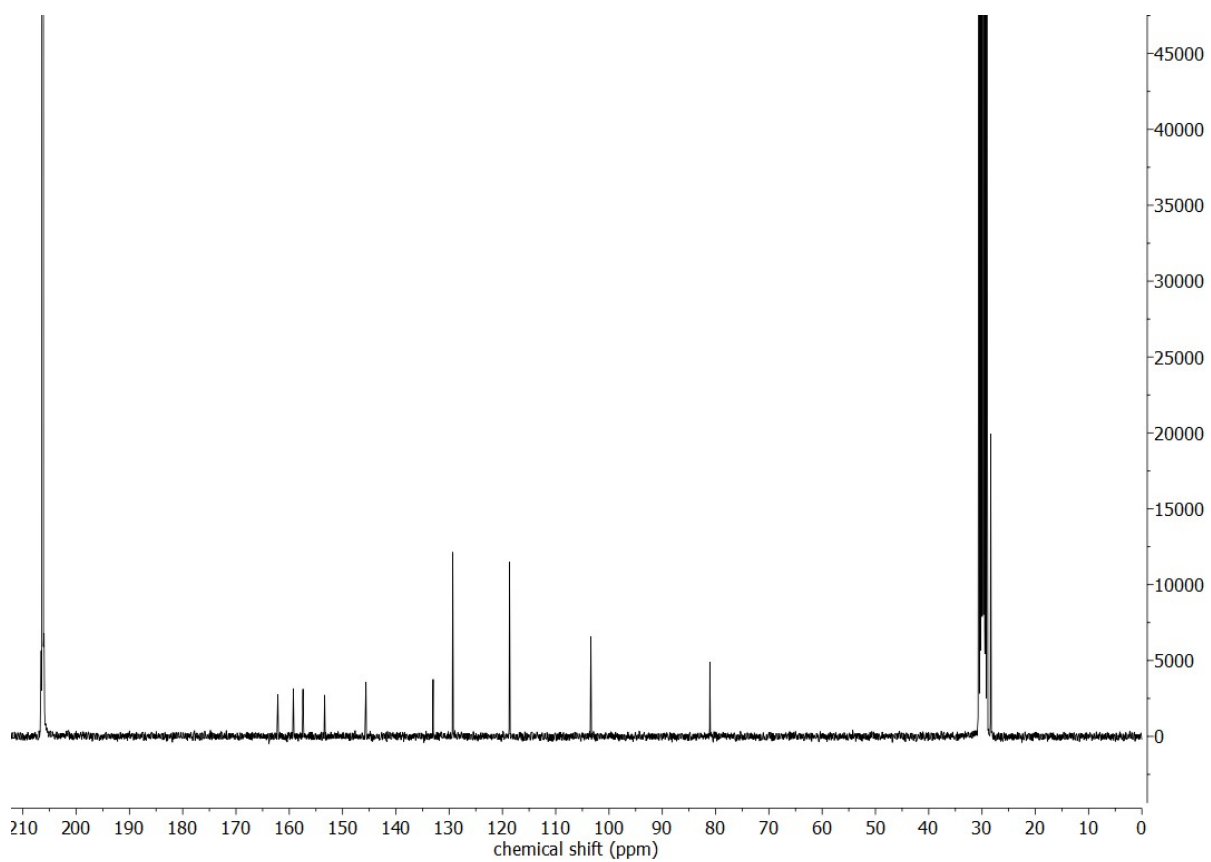


Figure S7: ESI-MS (positive mode) of **3**.



**Figure S8:** <sup>1</sup>H NMR spectrum of 4.



**Figure S9:** <sup>13</sup>C NMR spectrum of 4.

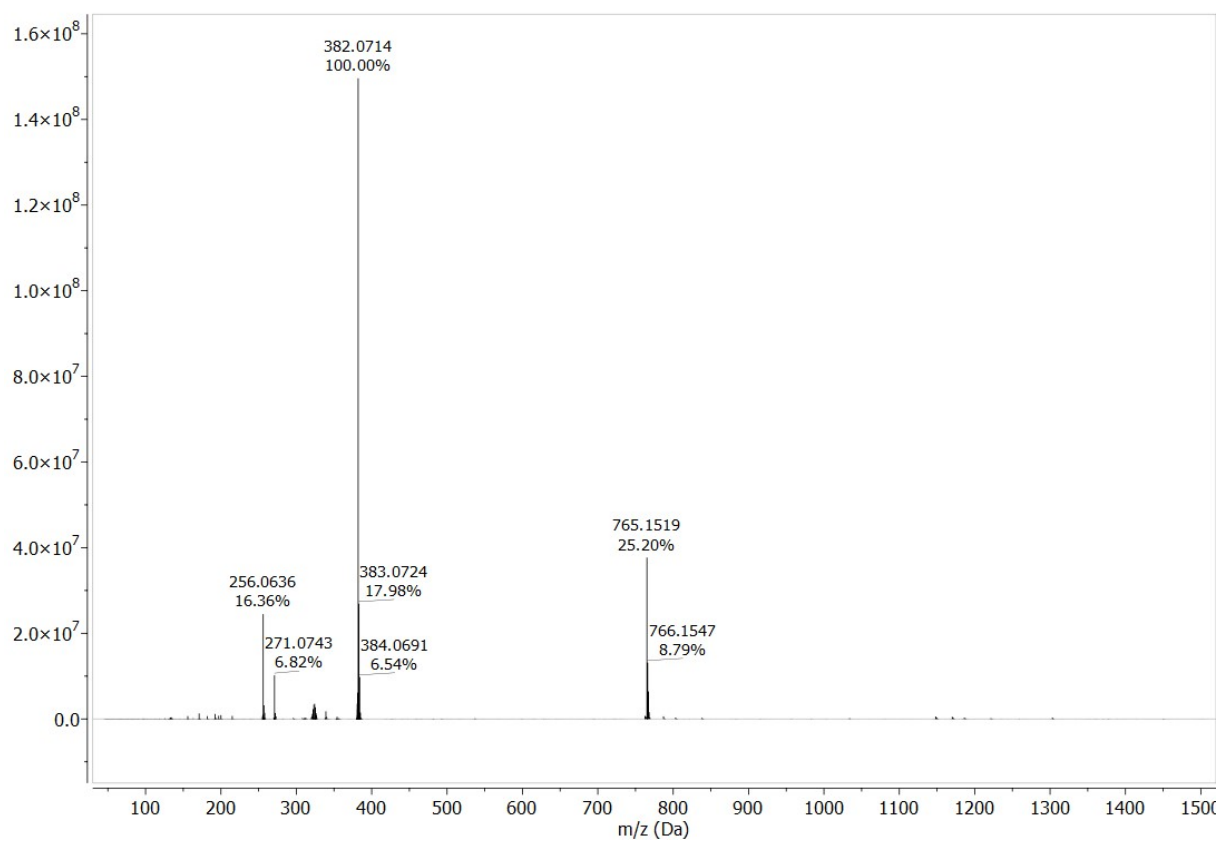


Figure S10: ESI-MS (negative mode) of 4.

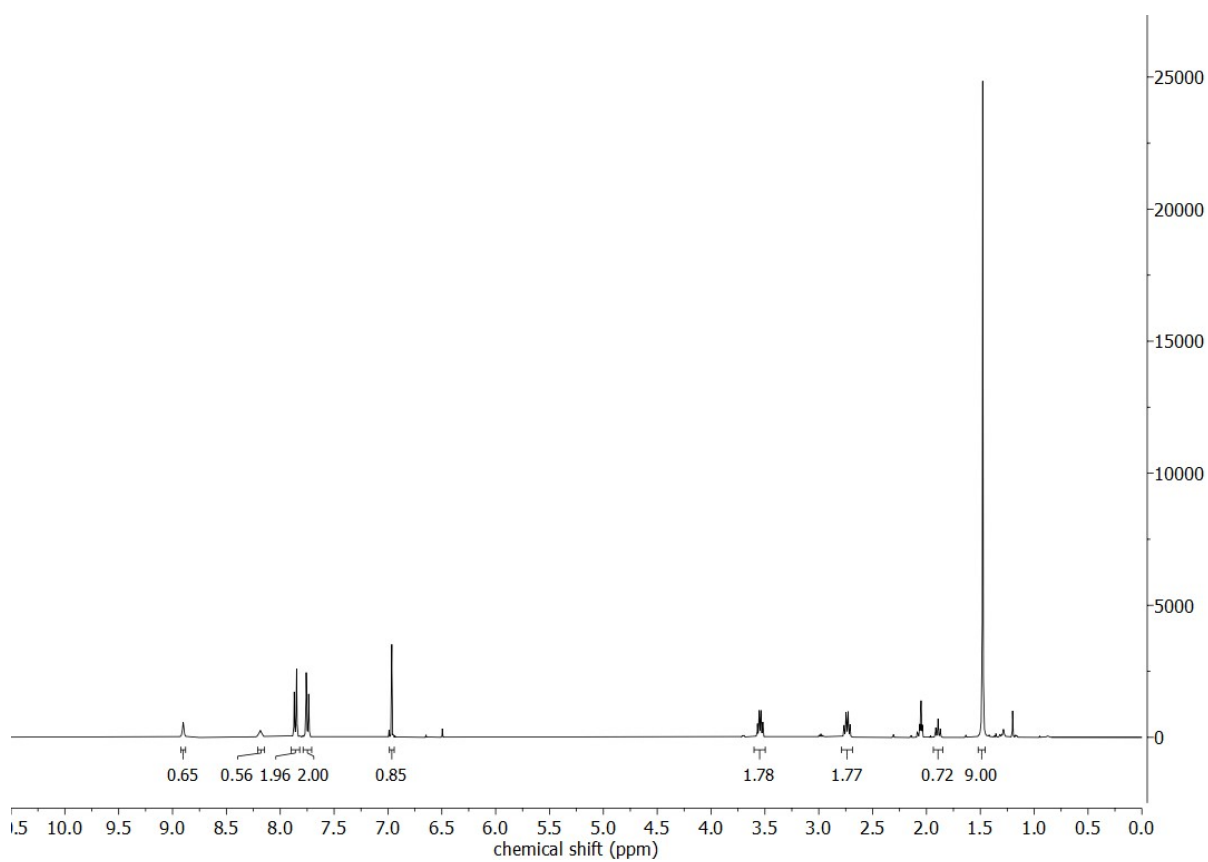


Figure S11:  $^1\text{H}$  NMR spectrum of 5.

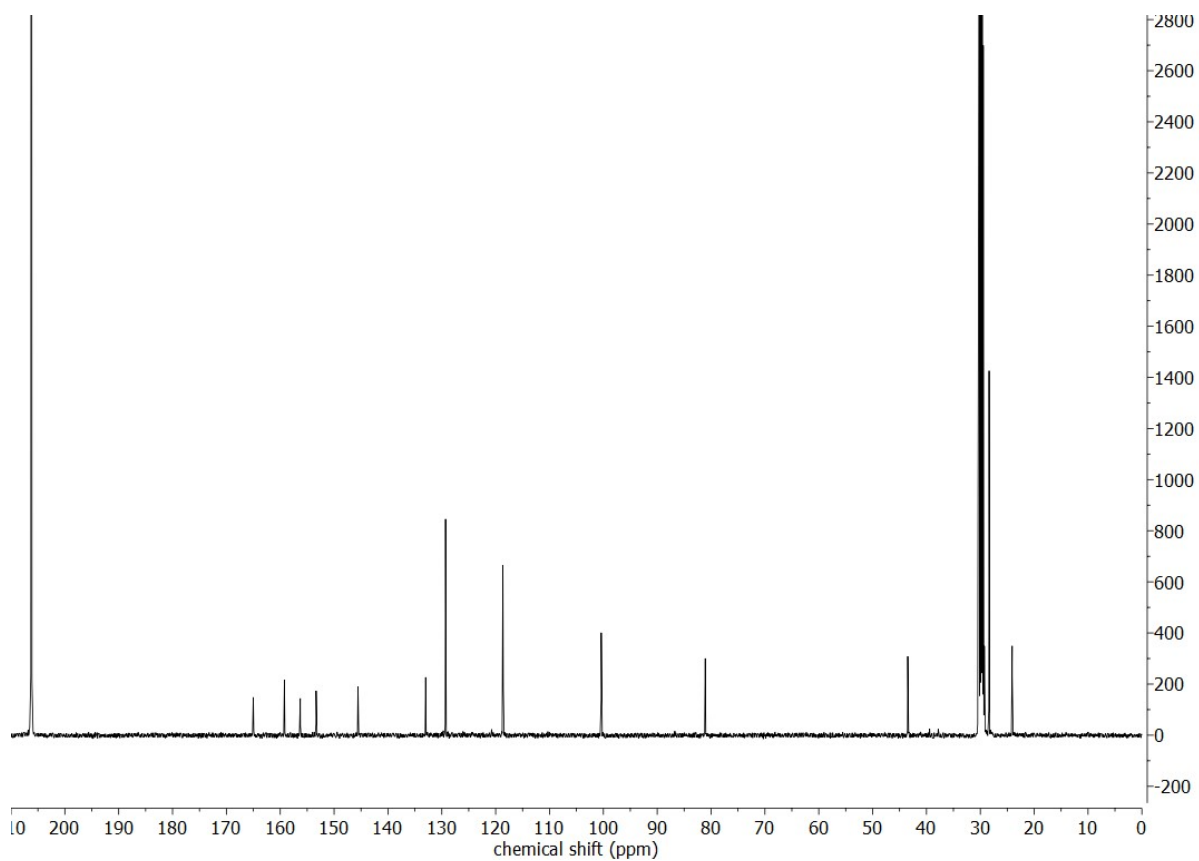


Figure S12:  $^{13}\text{C}$ -NMR spectrum of 5.

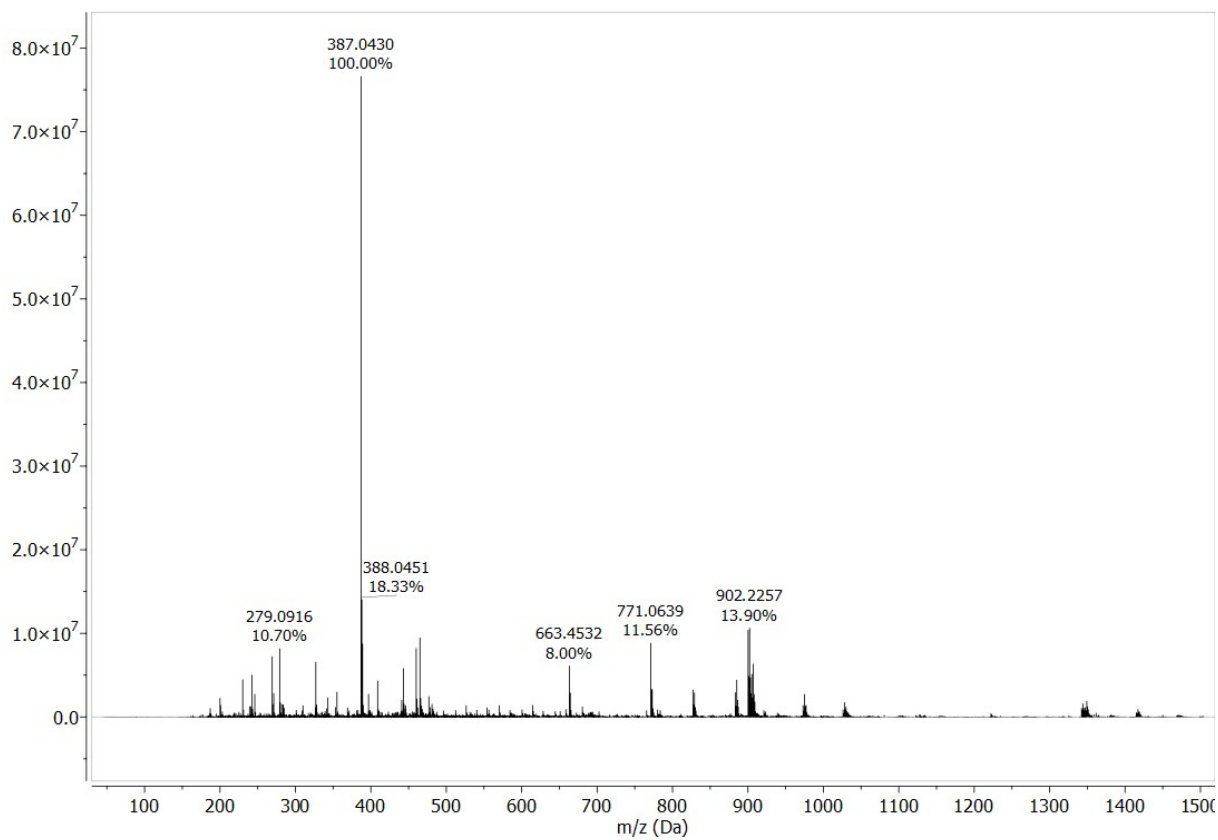
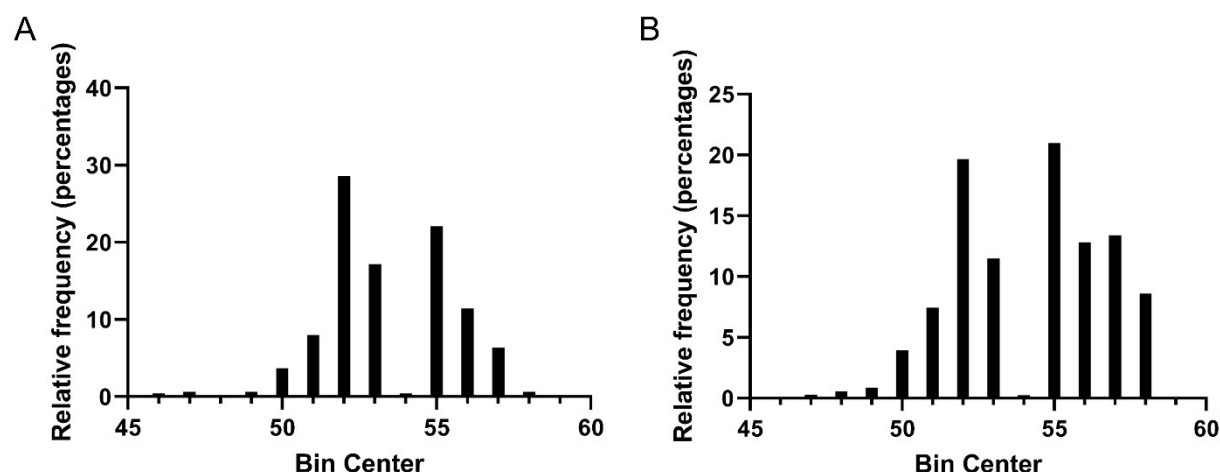


Figure S13: ESI-MS (positive mode) of 5.

#### 4. Size distribution of hydrogel microparticles after synthesis



**Figure S14:** Bright field microscopy analysis of hydrogel particle diameter. Measurements were performed according to the extended experimental section (1.3). Particle diameter size distribution is given in  $\mu\text{m}$ . A. Particles used for stability assessment towards functionalization with a mean particle diameter size of  $53.4 \mu\text{m} \pm 1.9 \mu\text{m}$  ( $n = 489$ ). B. Particles used for stability assessment towards acetone and HCl with a mean particle diameter size of  $54.2 \mu\text{m} \pm 2.3 \mu\text{m}$  ( $n = 687$ ).

#### 5. Fluorescence-based analysis of SMXder coupling to PEG hydrogel microparticles

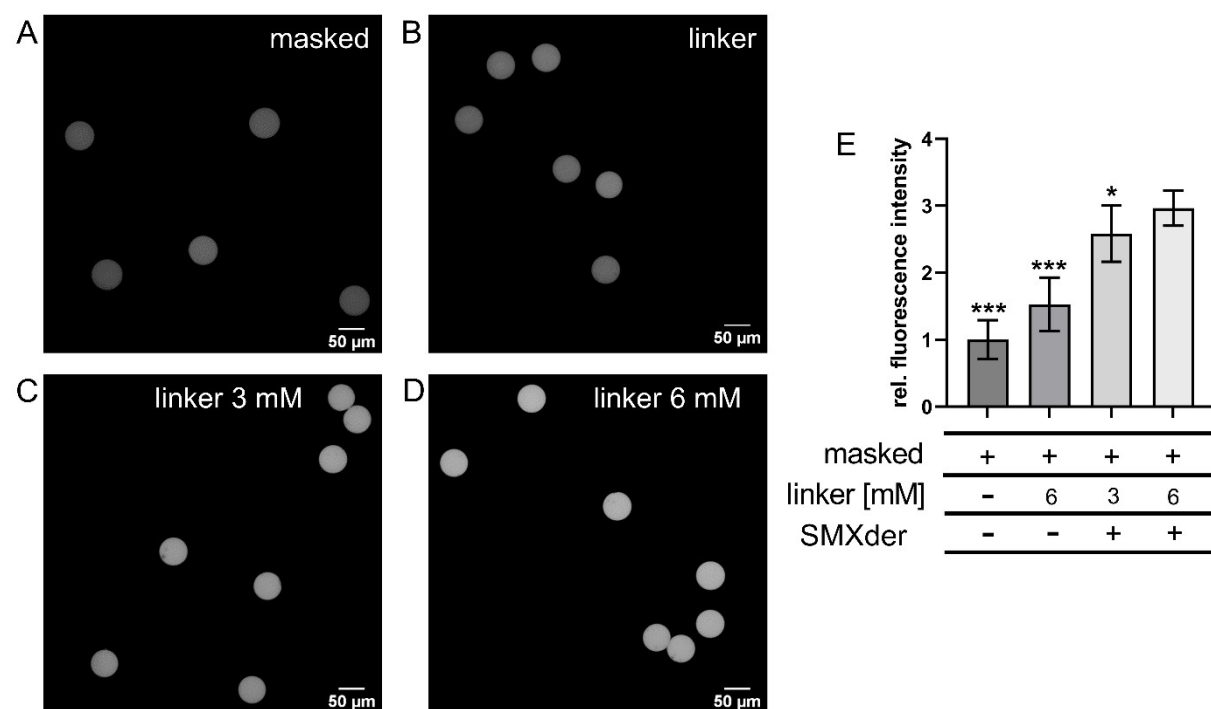


**Figure S15:** Fluorescence-based analysis of SMXmod coupled to hydrogel microparticles using different linker concentrations. Particles in all conditions were FITC stained after functionalization and masking. A: Hydrogel microparticles after masking with N-methyl maleimide. B: Hydrogel microparticles functionalized with 1,11-bis(maleimido)-3,6,9-trioxaundecane linker (6 mM) and masked with N-methyl maleimide. C + D: Different concentrations of 1,11-bis(maleimido)-3,6,9-trioxaundecane linker, namely 3 mM and 6 mM, were coupled to particles followed by binding of SMXmod (6 mM) and masking with N-methyl maleimide as the last step. E: Relative fluorescence intensity of at least 90 particles for each condition, normalized to unfunctionalized, masked and FITC-stained hydrogel microparticles (A) and shown as the mean  $\pm$  SD.

## 6. Stability assessment of hydrogel microparticles towards SMXder functionalization process and solvents

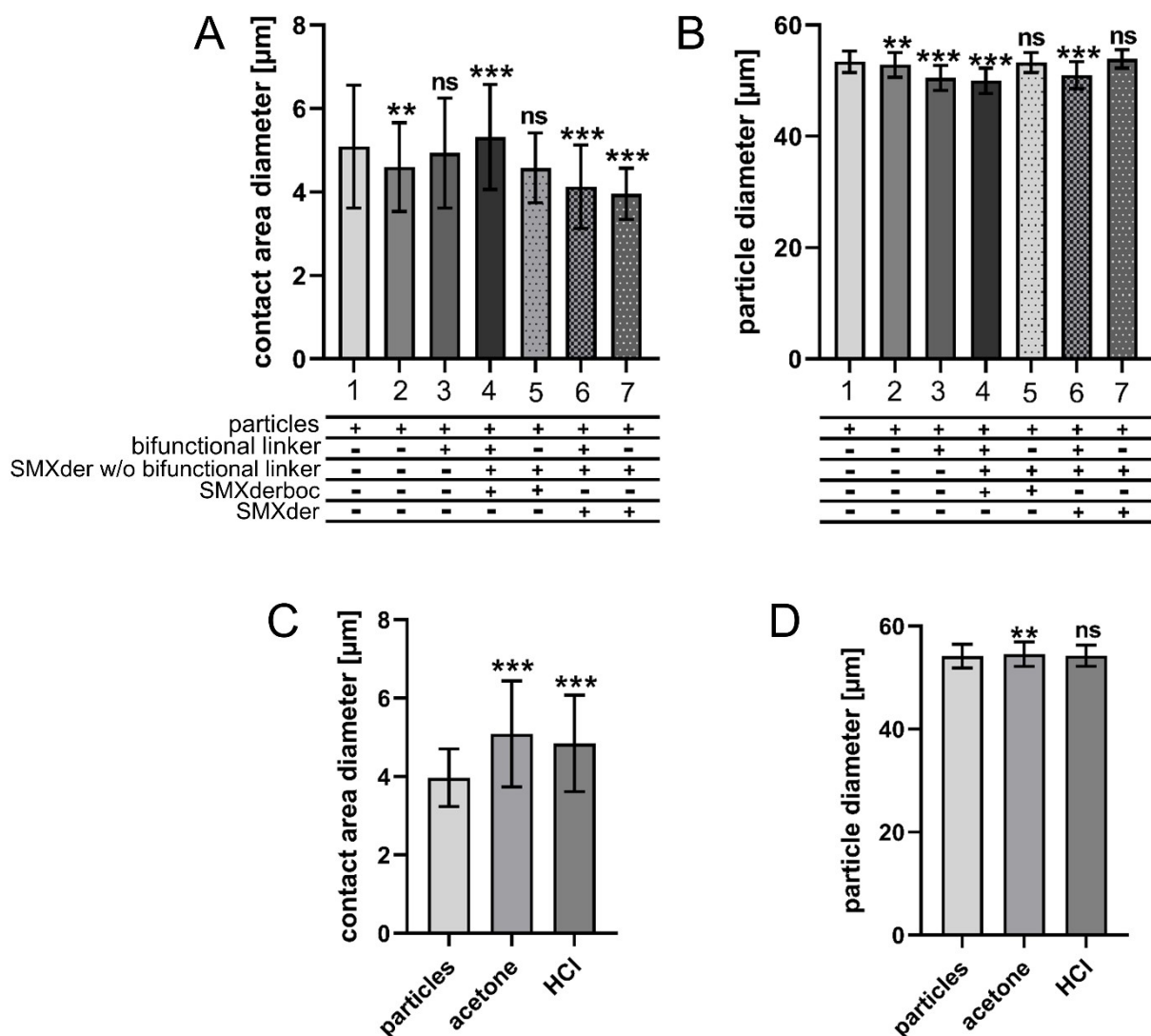


**Figure S16:** Stability analysis of hydrogel microparticles towards SMXmod coupling and the solvents acetone and HCl. (A) + (B) Functionalized hydrogel microparticles were analysed in regards to the size of the formed contact area on isopropanol cleaned glass surfaces (A) and in regards to their size via bright field microscopy (B). Statistical analysis was referred to the control condition (1). Data is shown as mean±SD. (1) control condition: particles after synthesis in Millipore water with a contact area diameter size of  $5.1 \mu\text{m} \pm 1.5 \mu\text{m}$  (A) and a particle diameter size of  $53.4 \mu\text{m} \pm 1.9 \mu\text{m}$  (B). (2) unfunctionalized particles that were treated analogously to functionalized particles. (3) particles coupled with 6 mM 1,11-bis(maleimido)-3,6,9-trioxaundecane-linker to thiol groups on the particle surface. (4) particles functionalized with boc-protected SMXmod via 6 mM 1,11-bis(maleimido)-3,6,9-trioxaundecane-linker. (5) particles directly functionalized with boc-protected SMXmod via the introduced thiol group at the SMX isoxazole ring (without 1,11-bis(maleimido)-3,6,9-trioxaundecane-linker coupling). (6) + (7) functionalization conditions corresponding to (4) and (5), respectively, but with deprotected SMXmod. (C) Analysis of contact area size on isopropanol cleaned surface using RICM after 4 h treatment with acetone or HCl. (D) Evaluation of particle diameter via bright field microscopy after 4 h treatment with acetone or HCl. Statistical analysis was referred to the control condition (particles), that is particles after synthesis stored in Millipore water with a contact area diameter size of  $4.0 \mu\text{m} \pm 0.7 \mu\text{m}$  (C) and a particle diameter size of  $54.2 \mu\text{m} \pm 2.3 \mu\text{m}$  (D). Data is plotted as mean±SD. P-values of the statistical analysis are indicated as  $P < 0.001$  (\*\*\*),  $P < 0.002$  (\*\*),  $P < 0.033$  (\*).

## Notes and references

- 1 M.-M. Zhan, Y. Yang, J. Luo, X.-X. Zhang, X. Xiao, S. Li, K. Cheng, Z. Xie, Z. Tu and C. Liao, *Eur. J. Med. Chem.*, 2018, **143**, 724–731.
- 2 K. Matsumoto, S. Hashimoto and S. Otani, *J. Chem. Soc. Chem. Commun.*, 1991, 306.
- 3 M. Gabler and M. Schubert-Zsilavec, *Molecules*, 2011, **16**, 10013–28.
- 4 A. Edelstein, N. Amodaj, K. Hoover, R. Vale and N. Stuurman, *CP Molecular Biology*, 2010, **92**, 14.20.1-14.20.17.
- 5 C. A. Schneider, W. S. Rasband and K. W. Eliceiri, *Nat. Methods*, 2012, **9**, 671–675.